*Acta Geologica Polonica*, Vol. 65 (2015), No. 4, pp. 525–543
DOI: 10.1515/agp-2015-0023

# The OAE1a in Cuchía (Early Aptian, Spain): C and O geochemistry and global correlation

JOAQUÍN GARCÍA-MONDÉJAR[1], PEDRO A. FERNÁNDEZ-MENDIOLA[1] and HUGH G. OWEN[2]

[1]*Department of Stratigraphy and Palaeontology, Universidad del País Vasco, Facultad de Ciencia y Tecnología, PO Box 644, E-48080, Spain.*
*E-mails: joaquin.garciamondejar@ehu.es; kepa.fernandezmendiola@ehu.es*
[2]*Natural History Museum of London, Department of Earth Sciences, Cromwell Road, London SW7 5BD, UK.*
*E-mail: hugh243@btinternet.com*

ABSTRACT:

García-Mondéjar, J., Fernándes-Mendiola, F. and Owen, H.G. 2015. The OAE1a in Cuchía (Early Aptian, Spain): C and O geochemistry and global correlation. *Acta Geologica Polonica*, **65** (4), 525–543. Warszawa.

C-isotopes, TOC and O geochemical data from the lower Aptian Cuchía section in the western Basque-Cantabrian basin (BCB) allow an accurate delimitation of the OAE1a-equivalent and its geochemical Menegatti´s segments, a detailed $\delta^{13}C_{carb}$ correlation with regional and interregional sections, and a high-resolution construction of TOC and bulk-rock $\delta^{18}O_{carb}$ curves and their interpretation. The $\delta^{13}C_{carb}$ values range from -2‰ and +4‰ (VPDB). They agree with previous data from the eastern BCB sections (Aralar) confirming the ammonite age of the OAE1a in the Basque-Cantabrian basin: *Deshayesites forbesi, Deshayesites deshayesi,* and *Deshayesites deshayesi-Dufrenoyia furcata* transition Zones. Interregional $\delta^{13}C_{carb}$ correlation with pelagic (Cismon, Italy, and Mid-Pacific Mountains, DSDP Site 463) and neritic (Roquefort-La Bédoule, France) core sections, reveals a common profile of a wide negative excursion characteristic of the OAE1a. It consists of a double trough separated by a flat relative maximum, with two negative spikes in the upper trough of neritic sections. TOC absolute values range from 0.12% to 1.37%. Segments of the TOC curve with persistent low values closely correspond with descending segments of the $\delta^{13}C_{carb}$ curve, and are attributed to lesser organic productivity in the BCB. Detailed bulk-rock $\delta^{18}O_{carb}$ data (-5.71‰ to -1.05 ‰ PDB) and variation curve show two main positive O-isotope shifts and three minor positive inflections, within a general negative trend characteristic of the OAE1a. The two major positive shifts correspond to both shallowing upwards sequences and the lowermost can be related to a eustatic sea level fall. Independent interregional correlation of the O-isotope shifts with C-isotopes supports their interpretation as punctuating colder events within a general warming trend.

**Keywords:** Cretaceous; Aptian; Basque-Cantabrian Basin; C-O isotopes; TOC.

## INTRODUCTION

Correlation of sedimentary rock sequences is a key element to palaeoenvironmental interpretation of ancient geological events. If correlation fails, rocks of different ages are wrongly considered coeval and building hypothesis and models lead to false interpretations. Extreme caution is necessary to correlate sequences within a basin or among distant basins. The OAE1a event is usually determined by a specific carbon isotope signature in combination with biostratigraphy (ammonites, nannoconids, foraminifera), facies (TOC-enriched series) and events (Osmium events, nannoconid crises) that can help to prove isochroneity between different areas.

Aptian sedimentary and palaeoenvironmental changes are related traditionally to global greenhouse climate changes influenced by extensive volcanism and superplume episodes (Larson and Erba, 1999; Jones and Jenkyns, 2001; Méhay *et al*. 2009; Tejada *et al*. 2009; Erba *et al*. 2010; Bottini *et al*. 2013). Environmental changes are attributed to warming at the sea-bottom that could have enhanced gas hydrates dissociation (e.g. Jahren *et al.* 2001; Wagner *et al.* 2007; Méhay *et al.* 2009). Rising atmospheric $CO_2$ is temporarily linked to intensive weathering, decreasing carbonate sedimentation, and weak ventilation of marine deep-waters (Arthur and Premoli Silva, 1982; Herrle *et al.* 2003). Surface water productivity periodically increased, and together with monsoons influenced nutrient runoff, precipitation rates and upwelling (Herrle *et al*., 2003). The impact of Aptian climate on biotas is summarized for nannoconids (Erba 1994), foraminifers (Premoli Silva *et al.* 1999; Moullade *et al.* 2002), radiolarians (Erbacher and Thurow 1995) and dinocysts (Wilpshaar and Leereveld 1994). Aptian climate and palaeoceanographic impact on sediments is also recorded by carbon isotopes (e.g. Menegatti *et al*. 1998) and organic matter (Schlanger and Cita 1982; Arthur *et al*. 1990; Heimhofer *et al*. 2004).

In this paper we provide high-resolution chemostratigraphic data from the Lower Aptian Cuchía section in the western Basque-Cantabrian Basin (BCB) mixed carbonate-terrigenous section (García-Mondéjar *et al*. 2015) (Text-fig. 1). This section reveals a chemostratigraphic signature equivalent to that of Selli Level and the OAE1a. The detailed $\delta^{13}C_{carb}$ curve improves the OAE1a correlation with Aralar (eastern BCB, Millán *et al*. 2009, 2011) and Cuchía (Najarro *et al.* 2011). New TOC and O-isotope curves are correlated at regional and interregional scales, giving precision to the timing of palaeoceanographic and palaeoclimatic changes affecting the Earth during the Early Aptian. Carbon and oxygen-isotope curves together with TOC absolute values and their variations for Cuchía (Text-fig. 2) are correlated among coeval sections of the BCB (Text-fig. 3) and with other basins around the world (Text-fig. 4). TOC and oxygen isotopes analyses support common interregional stratigraphic and geochemical signals (Text-figs 5, 6).

We delimit precisely the boundaries of the OAE1a in Cuchía, through a detailed comparison with the Lower Aptian reference section of the Cismon core (Apticore Unit 4, 18.77–23.68 m) (Selli Level, Erba *et al.* 1999), Italy. Here we include the first black shale bed within the Selli Level in accordance with Erba and subsequent authors. We especially compare the Cuchía $\delta^{13}C_{carb}$ curve with the curve of Erba *et al*. (2010, fig. 2), which showed an original photograph of the split core and a close-up view of the lowermost black shale bed.

Menegatti *et al.* (1998) recognized segments in the $\delta^{13}C_{carb}$ curve. According to these authors the Selli Level, generally accepted to represent the OAE1a, comprised segments C4 to C6 of the curve, based on two outcrop sections: Roter Sattel (Switzerland) and Cismon (Italy). Segment C3 in Cismon corresponding to a first black shale bed (Menegatti *et al.* 1998, fig. 3, bed at 267 m height) occurred below the Selli Level. Subsequent studies in the

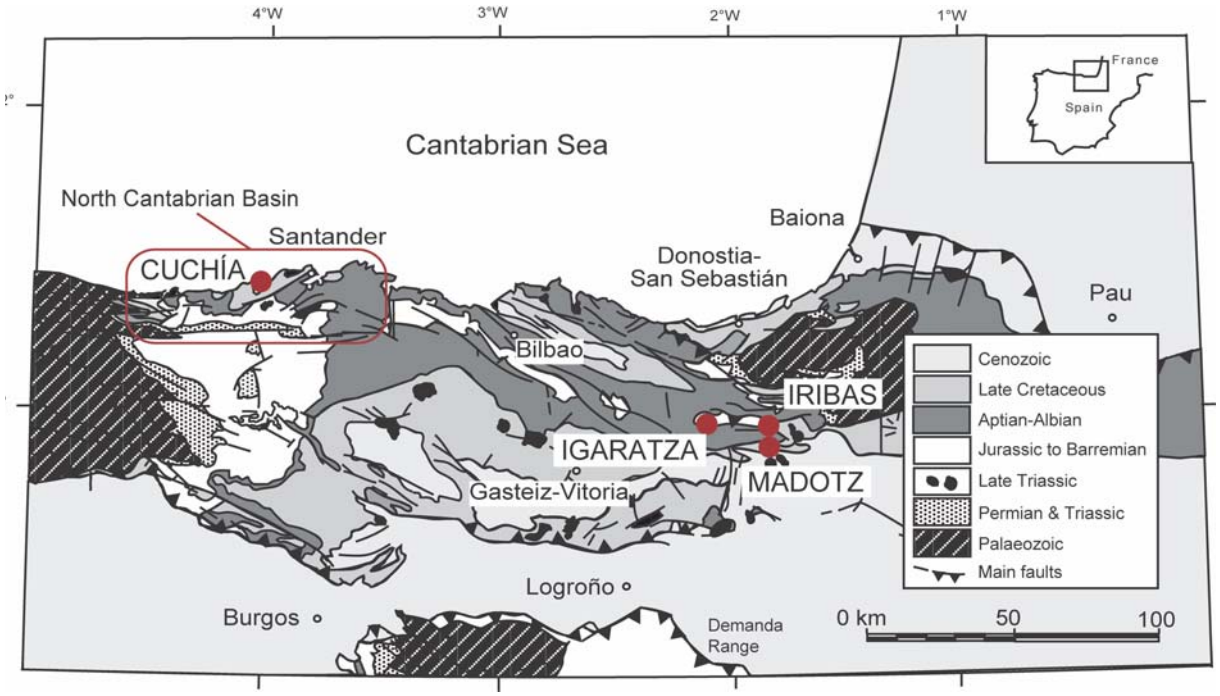


Text-fig. 1. Location of the studied sections of Cuchía (western part) and Igaratza, Madotz and Iribas (eastern part) in the Basque-Cantabrian Basin, northern margin of Iberia and south of the Cantabrian Sea

Cismon core section (Apticore work) included the first black shale bed located at the height 23.68 m within the Selli Level (Erba *et al.* 1999, fig. 3; Erba *et al.* 2010, fig. 2). Therefore the first black shale bed of the Selli Level from the Cismon core section corresponds to the Menegatti's segment C3 of the $\delta^{13}C_{carb}$ curve, and this segment has since been considered to be the base of the OAE1a by many authors (e.g. Erba *et al.* 1999; Méhay *et al.* 2009; Erba *et al.* 2010; Erba *et al.* 2015). Other works on the Cismon core section omitted the first black shale bed at 23.68 m. Thus they considered segment C3 of the Menegatti *et al*. (1998) curve to be below the Selli Level, and consequently below the OAE1a interval (e.g. Keller *et al.* 2011, fig. 2; Giorgioni *et al.* 2015, fig. 2).

Another core section of the lower Aptian from Roquefort-La Bédoule (SE France) is considered in this study and its $\delta^{13}C_{carb}$ curve interpreted in terms of the Menegatti´s segments (e.g. Lorenzen *et al.* 2013; Moullade *et al*. 2015). The section lacks TOC-rich beds and OAE1a identification relies on geochemistry and biostratigraphy, as in the case of Cuchía described here. Identification of the Menegatti's segments in Roquefort-La Bédoule section curve is not straightforward, and we give an alternative interpretation of the existing one using a correlation with the Cuchía neritic section and other pelagic sections. We also make an updated interpretation to the Menegatti's segments of the Cuchía section as proposed by Najarro *et al.* (2011).

## METHODS

The Cuchía stratigraphic section located west of Santander (Text-fig. 1) was investigated along 130 m of the lower Aptian succession (Text-figs 2 and 3). The Umbrera, Patrocinio and San Esteban Formations of this section were sampled metre by metre for carbon and oxygen-isotope analyses (Text-fig. 2). Powders were extracted from 130 samples of limestones, marls and calcareous lutites, to enable $\delta^{13}C_{carb}$ and $\delta^{13}C_{org}$ analysis. A micro-drill was used in order to avoid large detrital fragments and/or diagenetic calcite from veins.

The inorganic carbon and oxygen measurements were made with the Finnigan MAT 251 mass spectrometer at the Leibniz Laboratory, Kiel University (Germany). The instrument is coupled on-line to a Carbo Diel Device (Type I prototype). Samples were reacted by individual acid addition (99% $H_3PO_4$ at 73ºC). Standard external error is better than ±0.07% and ±0.05% for δ180 and $\delta^{13}C$, respectively. The instrument is calibrated with the international standard NBS19. The isotope values are reported in the conventional delta notation with respect to V-PDB.

The organic carbon measurements were made on bulk rock samples from marls and lutites. More than 5g of material were treated with HCL acid (2M) during 24h to completely removing any carbonate minerals. A few milligrammes of decarbonated powder were weighed in tin capsules and measured using a Thermo-Finnigan Flash EA112 Elemental Analyzer, linked to a Delta plus mass-spectrometer (Thermo-Finnigan). The reproductivity of the measurements based on replicate standards was ±0.1% for $\delta^{13}C$. The instrument is calibrated with the international standard NBS22 and IAEA-CH-6, and the isotope relations are expressed as per mil (‰) deviation from the Vienna Pedee Belemnite (VPDV). Analysis was carried out in the Laboratory of Services for Research Assistance from University of A Coruña (Spain). A first report of the results of these measurements was shown graphically in García-Mondéjar *et al*. (2015, fig. 5).

For TOC determination the same samples as for $\delta^{13}C_{org}$ analysis were treated with HCl at 80% to dissolve carbonate minerals and 15 mg of powder was taken (wt.%). The samples were introduced within a Carlo Erba-EA1108 Elemental Analyzer calibrated against the standard aspartic acid and urea. Precision of the analyses for replicate samples and standards was ±0.03%. Analyses were made in the Laboratory of the Research Assistant Services from University of A Coruña, amounting to a total of 72 samples.

## GEOLOGICAL SETTING

The Basque-Cantabrian Basin evolved closely associated with the Bay of Biscay ocean-floor spreading zone. Sea-floor spreading in the western Bay of Biscay began in the Early Aptian and progressed towards the East, up to the latest Santonian (e.g., Montadert *et al.* 1974; Wiedmann *et al.* 1983; Olivet 1996). Within this extensional scenario several sedimentary basins developed on the tectonically active North Iberian margin, often in half-graben configurations (Wilmsen 2005). Synsedimentary tectonics during Aptian-Albian times was the main driving control on the stratigraphic architecture and facies distribution (García-Mondéjar 1989, 1990).

An E-W 50 × 100 km extensional basin (NCB, North Cantabrian Basin, Wiese and Wilmsen 1999), developed on the North Iberian margin as a result of mid-Valanginian extensional movements. This NCB halfgraben basin was separated from the more subsident Basque Basin domain in the east by the "Río Miera Flexure" (Feuillée and Rat 1971). To the south, the NCB was bounded by the Cabuérniga Ridge (an

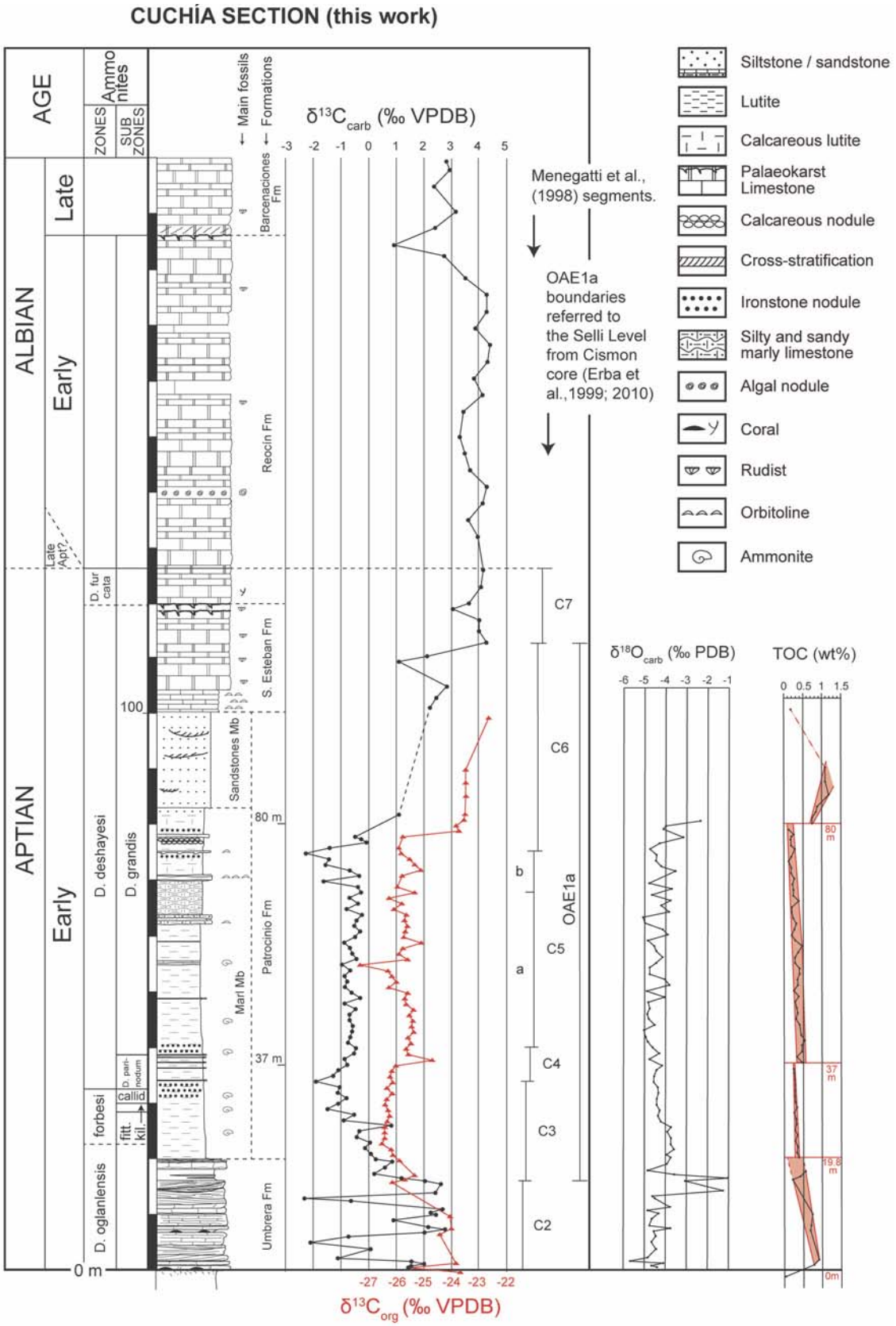


Text-fig. 2. Lithostratigraphy, age and geochemistry ($\delta^{13}C_{carb}$, $\delta^{13}C_{org}$, $\delta^{18}O_{carb}$ and TOC) of the Cuchía section

east-west trending horst structure formed of Palaeozoic and Triassic rocks) and by the Asturian Massif (Wilmsen 2005). To the west, the NCB was linked to the Asturian Cretaceous Basin. The NCB northern boundary is the "Liencres High" (Wiese 1995) representing the crest of a tilted block (Santander Block, Wilmsen 1997).

Sedimentation occurred in subtropical palaeolatitudes of 25–30°N (Masse 2000), and the Early Aptian reflects warm palaeoclimatic conditions (e.g., Kemper 1982). The facies discussed in this study correspond of the Early Aptian 'first biosedimentary system' of Pascal (1982).

The pioneering work of Mengaud (1920) provided the first stratigraphic description and ammonite content. Collignon *et al*. (1979) described the ammonite fauna, establishing the first biozonation. Wilmsen (2005) distinguished lithostratigraphic units and interpreted their sedimentology. Najarro *et al*. (2011) reorganized the Cuchía lithostratigraphy and dated the marls of the Patrocinio Formation as *Deshayesites weissi* Zone age (*Deshayesites forbesi* Zone in current terminology), based on ammonite identifications. Additionally, they interpreted the OAE-1a equivalent based on C-isotopes in the Patrocinio Formation and dated it in the *D. forbesi* ammonite Zone. This age has been reviewed, and a much wider OAE1a age from *D. forbesi, Deshayesites deshayesi* to *D. deshayesi-Dufrenoyia furcata* transition Zones is assigned (García-Mondéjar *et al.* 2015; this work).

## CARBONATE C-ISOTOPES

The measured bulk $\delta^{13}C_{carb}$ absolute values vary between +4.4 ‰ and -2.31‰ (Text-fig. 2). The Umbrera Formation shows oscillating low and high values. The maximum values make up the most characteristic signal of the curve, which shows a rapid decrease in the uppermost part of the formation starting at metre 16 (Text-fig. 2).

The Patrocinio Formation is characterized by overall negative $\delta^{13}C_{carb}$ absolute values. The base of this formation maintains the descending trend of the underlying Umbrera Formation to a first minimun spike at 34 m (-1.89‰). Small variations characterize the stretch between 38 and 68 m. A first negative trough in the curve is depicted from 17 to 35 metres (Text-fig. 2). The subsequent descending trend determines a second trough recorded from 68 to 78 m, with two negative spikes (-1.62‰ and -2.26 (Text-fig. 2). A rapid rise follows reaching +1.11‰ at the end of the Patrocinio marls at 82 m (Text-fig. 2).

The San Esteban Formation shows a rise to a maximum +4.27‰. The Albian Reocín Formation shows absolute values distributed uniformly around +4.0‰. Finally, the Upper Albian Barcenaciones Formation values oscillate between +2.0‰ and +3.0‰ (Text-fig. 2).

In summary, the shape of the $\delta^{13}C_{carb}$ curve described in the Umbrera and Patrocinio Formations (Text-fig. 2, 84 samples) is reminiscent of a previous curve from Najarro *et al*. (2011, fig. 6, 42 samples). We recognize a broad negative carbon-isotope excursion in the lower Aptian Patrocinio Formation between metres 20 and 80. This negative excursion contains two troughs made up of lighter values, respectively around metres 30 (trough 1) and 75 (trough 2) (Text-fig. 2). We discuss below that these spikes are significant in interregional correlation. We finally recognize a positive carbon-isotope excursion in the latest Early Aptian from metres 110 to 120 in the San Esteban Formation (Text-fig. 2).

## ORGANIC C-ISOTOPES

The measured bulk $\delta^{13}C_{org}$ absolute values vary between -27.3‰ and -22.6‰ (Text-fig. 2). In the lower part of the Umbrera Formation they define a relative maximum oscillating around -24.0‰. In the upper part of the same Formation absolute values show a descending trend to around -26.0‰, which continues to a first minimum spike (-26.5‰) already at the base of the Patrocinio Formation. The next interval is characterized by a gently rising trend up to values consistently around -25.5‰.

A new negative spike follows (-27.3‰) and subsequent values rise again and remain with repeated oscillations between -26.0‰ and -25.0‰, up to the end of the Marl Member of the Patrocinio Formation. A very rapid jump from -25.8‰ to -23.7‰ values is shown at 77.6 m in the section (Text-fig. 2). The last interval of the Formation corresponds to the Sandstone Member, with absolute values vertically maintained at -23.4‰ in the lower part, and a last higher value of -22.6‰ at the very top of the Formation.

The $\delta^{13}C_{org}$ curve shows a significant and broad negative excursion from metre 10 to 77, including a well-marked first trough (metre 17 to 37) equivalent to that shown in the $\delta^{13}C_{carb}$ curve. Both the $\delta^{13}C_{carb}$ and $\delta^{13}C_{org}$ curves from Cuchía present highly concordant trends (Text-fig. 2), pointing to a reliable C-isotope signal.

## TOC CONTENT

The TOC content of 72 samples from the Umbrera Fm (marly intervals) and the Patrocinio Fm has been de-

termined (Text-fig. 2). The values obtained range from 0.12% to 1.37%, with the maximum corresponding to lutites from the Sandstone Member of the Patrocinio Formation, and the minimum to the Marl Member of the same Formation.

The curve with all absolute TOC values shows four distinct intervals. They are separated by three abrupt excursions in the section: 1) towards lower values (19.8 m), 2) towards higher values (37 m), and 3) towards higher values again (80 m) (Text-fig. 2). In order to emphasize the four intervals, minimum and maximum envelopes of the data points have been drawn.

## OXYGEN ISOTOPES

$\delta^{18}O$ values of the Cuchía section range from a maximum of -1.05‰ in the upper part of the Umbrera Formation to a minimum of -5.71‰ in the lower part of the same Formation. However most of the measurements oscillate between -3.50‰ and -5.00‰ (Text-fig. 2). Measurements were made at every metre in an 80 m segment of the Cuchía section (Text-fig. 2). The $\delta^{18}O$ curve in Figure 2 shows a minimum excursion from 1.5 to 13 m in the basal Early Aptian (*Deshayesites oglanlensis* Zone). Values then rise sharply to a maximum at 16 m followed by a second maximum at 19.5 m.

The next interval of the curve (*D. forbesi* and *D. deshayesi* Zones) shows first a decreasing trend, and then low-amplitude oscillations, starting at 21.1 m and ending at 37 m. Second, a large trend with wider (1 ‰) oscillations, between 37 and 62 m. Third a last rising trend in two steps from 63 to 65 m and from 75 to 79 m.

The $\delta^{18}O$ absolute values obtained in Cuchía are low in comparison with others from other Early Aptian sections. For instance, in the Cismon core, Erba *et al*. (2010) describe values oscillating between -0.5‰ and -3.0‰ and in Cassis-La Bédoule (Kunht, Holbourn and Moullade 2011) similar oscillations vary between -1 .5‰ and -2.5‰. However most Cuchía values are higher than -5‰, which is the figure taken in recent sediments as the lower limit of marine carbonates (James and Choquette 1990).

## THE OAE1a IN THE BASQUE-CANTABRIAN BASIN

The sedimentary and geochemical expression of the OAE 1a in the Cuchía section is now correlated with the data derived from the Igaratza and Madotz sections of the eastern end of the Basque Cantabrian basin.

### The OAE1a in Cuchía

The Cuchía section shows one of the thickest outcrop expressions reported in the world for the lower part of the OAE1a (Text-fig. 2). The base of the OAE1a is placed in a very sharp drowning surface at top limestones just after the beginning of the $\delta^{13}C_{carb}$ negative excursion (metre 16, Text-fig. 2), where it has an absolute value of 2.0 ‰, close to the 2.5‰ at base of the Selli Level in Cismon core (Erba *et al*. 2010). The Selli level is considered equivalent to OAE1a, following Erba *et al*. (1999, p. 388), Bottini *et al*. (2013, p. 583) and elsewhere. In Cuchía, the top of the OAE1a is placed where $\delta^{13}C_{carb}$ reaches values around +4‰ and stabilize (metre 112, Text-fig. 2) (top Selli Level, e.g. Erba *et al*. 1999). Intervals C3, C4, C5 (a and b new subsegments) and C6 of Menegatti *et al*. (1998) are included in the OAE1a following Erba *et al*. (1999) and subsequent authors. They have been differentiated through comparison with the Cismon section and core (e.g. Menegatti *et al*. 1998; Erba *et al.* 1999), as explained in detail below. Two troughs: C3-C4 and C5b-base C6 are distinguished, the last one characterized by a double negative spike (Text-fig. 2). Our work confirms the presence of the OAE1a equivalent in Cuchía (Najarro *et al.* 2011), and establishes a different base and new boundaries of the internal Menegatti's geochemical segments. This permits for the first time a highly precise ammonite age attribution to the Menegatti *et al*. (1998) segments based on García-Mondéjar *et al*. (2015).

### Correlation of the OAE1a in Cuchía, Igaratza and Madotz

The OAE1a was geochemically identified in two sections of Aralar, in the eastern Basque-Cantabrian basin: Igaratza (Millán *et al.* 2009) and Madotz (Millán *et al.* 2011). In both cases ammonites procured biostratigraphic dating of the lower part of the OAE1a, namely segments C3, C4 and base of C5 of Menegatti *et al*. (1998). The section of Cuchía, located in the western part of the same basin (Text-fig 3) also with a well-identified OAE1a-equivalent by geochemical correlation, provided with a supplementary ammonite dating (García-Mondéjar *et al.* 2015). Apart from refining the information of Aralar the Cuchía data permits to extend the OAE1a throughout the whole BCB.

The three sections in Text-fig. 3 are correlated on the basis of key tie-points provided by ammonites-biozone boundaries where available, profile shape and comparison of absolute $\delta^{13}C$ values. The Igaratza and Madotz sections show the entire Early Aptian (500 m thick in

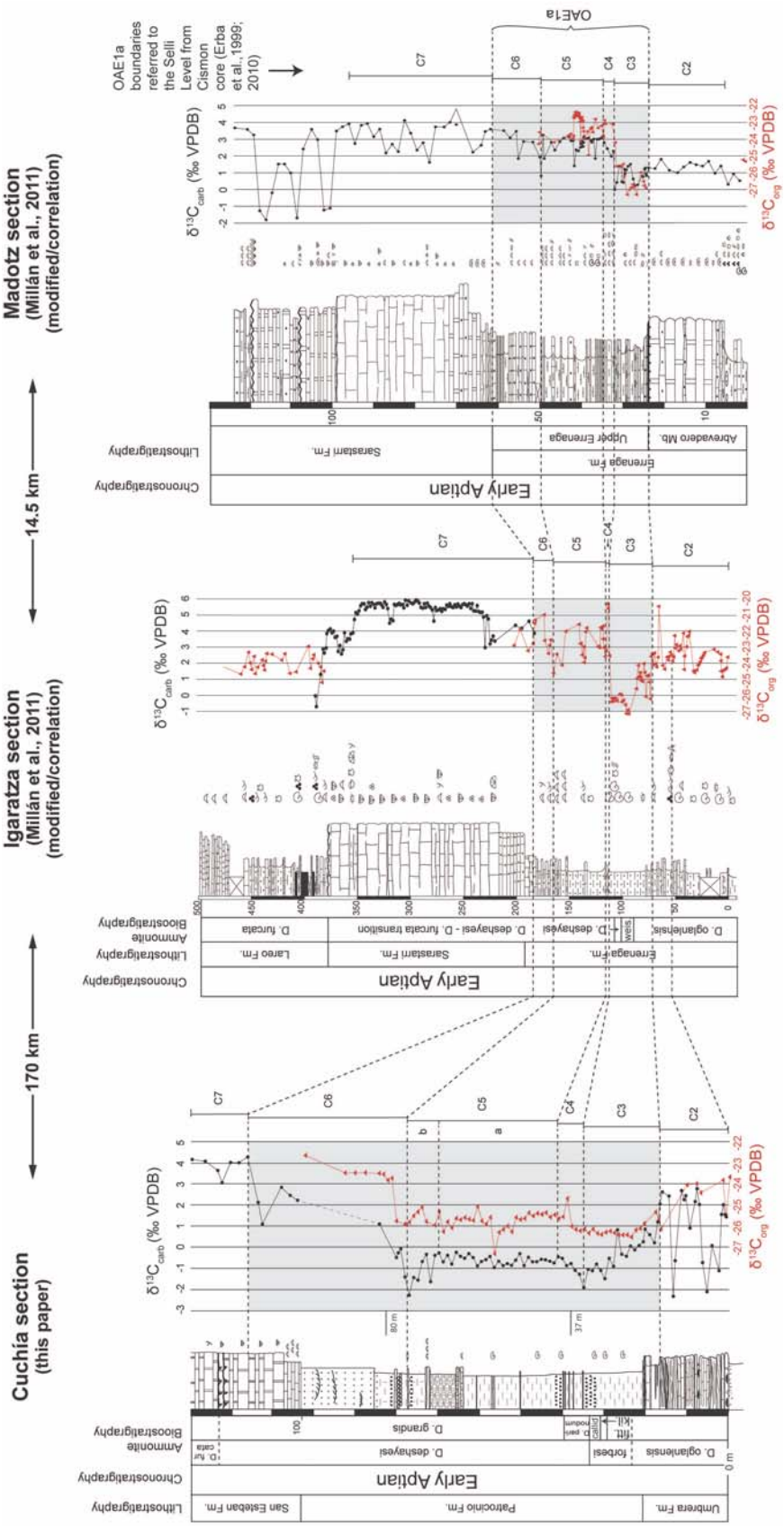


Text-fig. 3. Correlation of the early Aptian $\delta^{13}C_{carb}$ and $\delta^{13}C_{org}$ curves from Cuchia (this work) with those of Igaratza and Madotz sections. The two last curves (Millán *et al.* 2011) have been modified in segments C3 (Igaratza) and C4 (Madotz) to establish a better correspondence with Cuchia and Cismon core sections (See also Text-fig. 4). All sections have interpreted the *C2-C7* segments from Menegatti *et al.* (1998), with C3-C6 segments indicating the OAE-1a equivalent. The ammonites from Cuchia and Igaratza date the C3-C5 segments and those from the Madotz section date the C5 segment

Igaratza). The OAE1a is followed by a large positive excursion of $\delta^{13}C_{carb}$ values, close to 6‰ VPDB (Igaratza, C7 segment of Menegatti *et al.* 1998). The Cuchía section has, as the Igaratza section, an expanded base of the OAE1a but a reduced C7 segment owing to the presence of an important palaeokarst at top of San Esteban limestones (Text-figs 2 and 3).

This OAE1a internal organization in segments and the equivalence with Igaratza differs from that proposed by Najarro *et al*. (2011, fig. 6), as our C4-C5 intervals correspond to their C3 interval and they did not differentiate segment C6 (Text-fig. 2).

The geochemical correlation among the sections is coupled with the biostratigraphic correlation using ammonites. The sediments equivalent to the C3-C5 segments interval contain a large fauna of ammonites in Cuchía and Igaratza, dating it in the *D. forbesi*, *D. deshayesi* and lowermost part of *D. deshayesi-Dufrenoyia furcata* transition Zones. Therefore the segments C3, C4 and C5 of the OAE1a are well identified and correlated between Igaratza and Madotz (Aralar, eastern BCB). The Cuchía $\delta^{13}C_{carb}$ curve serves for a more accurate correlation with the Cismon core, such that the segment boundaries in Igaratza-Madotz sections have been slightly modified from those of Millán *et al*. (2011), which were compared between them using $\delta^{13}C_{org}$ values.

In figure 3 we show precisely that the base of C3 segment –base of the Selli Level equivalent- in Igaratza is differentiated in the descending part of the curve at a negative spike occurring before the most pronounced spike minimum. The C4 segment is slightly adjusted in Madotz (Text-fig. 3) to make it correspond with the rising trend of C4 in Cuchía, and with the similar rising trend segment in Cismon core (Text-fig. 4). Finally, the base of C6 segment is slighty lowered in Igaratza, to make it correspond with the equivalent minimum spike in all three locations of Cuchía, Madotz and Cismon core (e.g. Erba *et al*. 1999, for the latter). At least segment C5 and all segments above it (C6 and C7) correspond to the *D. deshayesi-D. furcata* transition Zones (Text-fig. 3).

The above underlines that even in thick sedimentary successions as in the Basque-Cantabrian basin, there is variation in the degree of representation of segments arising from local variations in the rate of sedimentation.

## INTERREGIONAL CORRELATION OF THE OAE1a

The exceptional thickness, ammonite biostratigraphy and carbon isotope signal (organic and carbonate) of the OAE 1a-equivalent in the Cuchía section, enable a high-resolution geochemical correlation with $\delta^{13}C$ curves from selected sections of the world. This is intended to facilitate correlation between neritic and pelagic both core and outcrop sections.

Comparisons are made with the Cismon core (N Italy, Erba *et al.* 2010), Roquefort-La Bédoule core (SE France, Lorenzen *et al.* 2013; Moullade *et al.* 2015) and DSDP site 463 in the Pacific Ocean (Bottini *et al*. 2013). All sections have been redrawn and enlarged in Text-fig. 4. We consider also the OAE1a boundaries established in the Cismon core reference section, i.e. the Selli Level boundaries (Erba *et al.* 1999).

### Cuchía-DSDP site 463 correlation

Recent research on the exceptional sets of interactions between the geosphere, biosphere and ocean-atmosphere system in the early Aptian has involved the use of Osmium isotopes to decipher the oceanic relationships of water masses (Tejada *et al.* 2009; Bottini *et al.* 2013). The geochemical record from the Pacific (DSDP 463) and the Tethys (Cismon core) reflect good coincidence in terms of carbon-isotope and $^{187}Os/^{186}Os$ curves, and provide important data for a causal link between development of the Ontong Java Plateau volcanism and establishment of seawater anoxia (op. cit.).

Correlation of the $\delta^{13}C_{carb}$ negative excursion of the Cuchía section and DSDP site 463 (Bottini *et al.* 2013) is represented in the central part of Text-fig. 4. In both sections there is a comparable trend of the carbon-isotope curves. The OAE1a at DSDP site 463 is characterized by a marked negative excursion from metres 614 to 625 (see Text-fig. 4). This broad excursion is correlated with the substantial negative trough from metres 16 to 112 in the Cuchía section (Text-fig. 2). Within the negative excursion of DSDP site 463 two further negative troughs are recognized. Trough-1 stands around metre 622.5 and trough-2 around metre 617.2. Similar prominent troughs, although less pronounced, can be recognized at parallel horizons in Cuchía, where trough-2 is further subdivided into a double negative spike (Text-fig. 4).

### Cuchía-Cismon core correlation

The overall negative inflection of the $\delta^{13}C_{carb}$ curve in DSDP site 463 (Pacific Ocean) and Cuchía is also recognized in the Cismon core from metres 18.8 to 23.8 (Text-fig. 4, right part), and correlation of the same excursion has been made between the Pacific and Italy cores independently using osmium-isotope curves (Bottini *et al.* 2013, fig. 1). The Pacific trough-1, within the general negative excursion (Bottini *et al*. op. cit.) is well recognized in the Cismon core (CIE interval) (Text-

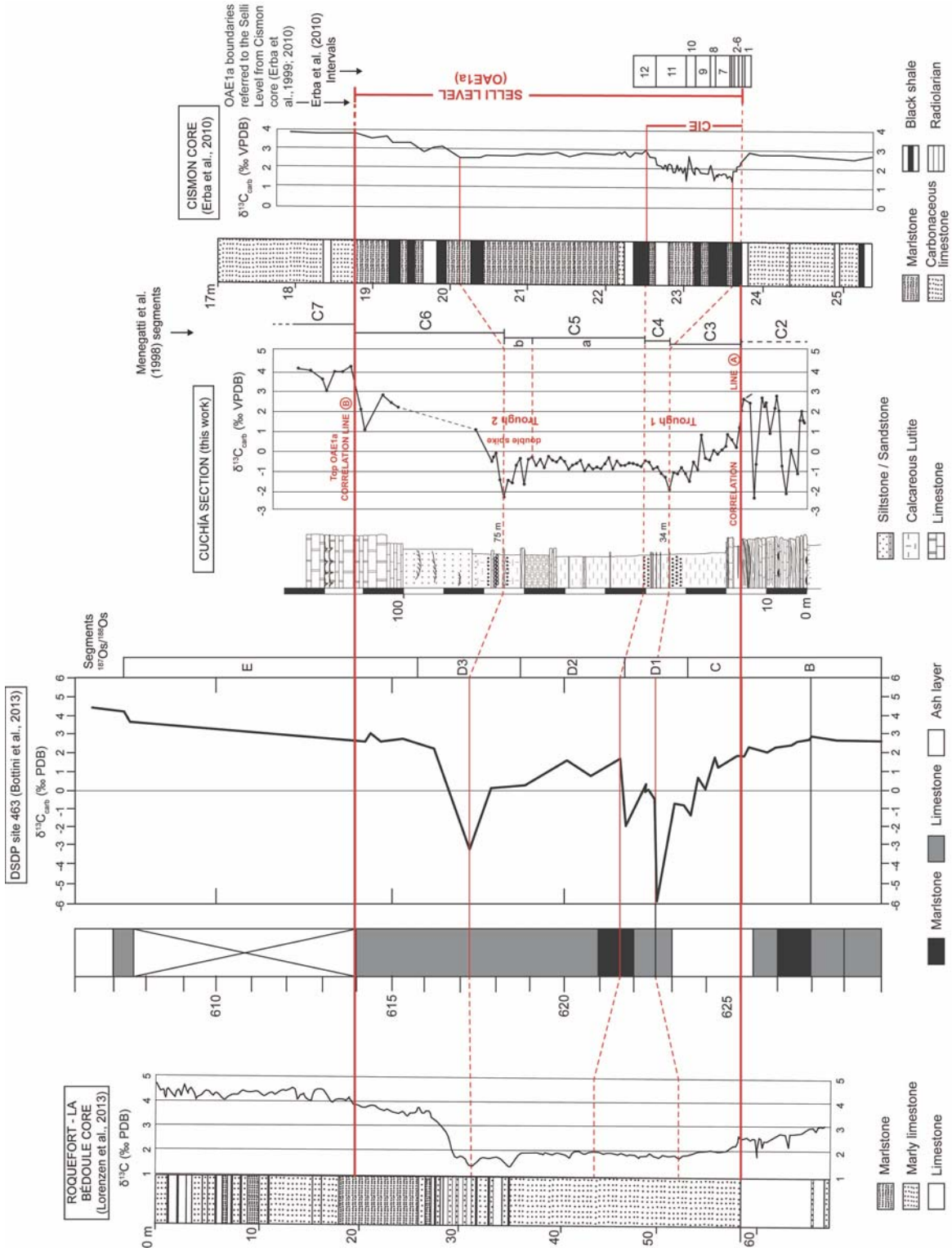


Text-fig. 4. Correlation of the $\delta^{13}C_{carb}$ curve from Cuchía section with similar curves from Cismon core (Erba *et al.* 2010), Roquefort-La Bédoule core (Lorenzen *et al.* 2013) and DSDP site 463 (Bottini *et al*. 2013). All curves have been redrawn and enlarged. Correlation lines A (carbonate crisis level) and B (top of the OAE1a) link curve points with equivalent absolute values and shifts of the $\delta^{13}C_{carb}$ trends, delimiting the Selli Level and the negative carbon-isotope excursion (CIE). In Cuchía and DSDP 463 sections the Selli-equivalent interval appears as a double negative trough in the curves. The second trough in Cuchía contains a double spike, as in the Roquefort-La Bédoule section. $^{187}Os/^{188}Os$ segments of Bottini *et al.* (2013) and CIE intervals of Erba *et al*. (2010) help to constrain the indirect correlation with Cuchía section

fig. 4). However the counterpart of trough-2 of the DSDP site 463 in Cismon core is much less prominent (see Bottini *et al.* 2013). We suggest that trough-2 equivalent can be situated around metre 20.2, where values define a faint negative trend (Erba *et al*. 2010).

In the Cismon core there is a key horizon at the base of the Selli level, defining the onset of a carbonate crisis (Erba *et al*. 2010). This horizon marks a decline in carbonate content, which was preceded by a significant nanoconid crisis. The base of the Selli Level has an equivalent surface in Cuchía marked by a sharp drowning episode at the level of correlation line A (Text-fig. 4). In both Cismon and Cuchía sections this surface corresponds to a small step in the first descending parts of their respective $\delta^{13}C_{carb}$ curves, inmediately after the beginning of their common negative excursion (Text-fig. 4). In Cismon the carbonate crisis level has a $\delta^{13}C_{carb}$ absolute value around 2.5‰ (Erba *et al.* 2010). The same equivalent level in Cuchía has an absolute value of 2‰.

In the Cismon core the negative trajectory of the curve begins from a $\delta^{13}C_{carb}$ absolute value around 2.9‰. This important shift point has been accurately identified in Cuchía, with a $\delta^{13}C_{carb}$ value of 2.67‰ (Text-fig. 4, just below correlation line A).

The negative trajectory of the curve in Cismon changes to positive trajectory around 1.5‰, and ends with a strong rising trend from approximately 2‰ to 3‰. The interval corresponding to this negative trajectory (CIE) is about 1.3m thick (Text-fig. 4). In Cuchía, the negative excursion equivalent to the CIE appears also as a trough (trough 1 in Text-fig. 4) representing 23 m in thickness.

The higher parts of the $\delta^{13}C_{carb}$ curves in both Cismon and Cuchía, from the top of the CIE to the top of the Selli Level, show rather parallel trajectories although with less data in Cuchía because the upper interval is dominated by the Patrocinio Sandstone Member (metres 83 to 100 in Text-fig. 4). In Cismon, the absolute values of this interval descend slowly from approximately 3.0‰ to 2.5‰, and they rise quickly to around 4‰. In Cuchía the absolute values descend with oscillations to around -2‰ and then they rise sharply to around 4‰ (Text-fig. 4).

## Cuchía-Roquefort/La Bédoule core correlation

The $\delta^{13}C_{carb}$ negative flexure of the Early Aptian identified in the previous sections is also represented in the Roquefort/La Bédoule core, from metres 19 to 58 (Lorenzen *et al.* 2013; Moullade *et al*. 2015) (Text-fig. 4, left part). In our interpretation the two troughs comprised in the negative excursion of the curve, identified in Cuchía and DSDP 463 site, are also recognized in the Roquefort section with 1.5-2 ‰ values. Trough -1 is less prominent and smoother in shape and lies around metre 52 in Text-fig. 4. Trough 2 is very prominent and, as in Cuchía, is subdivided into a double spike at the respective heights of 31.5 and 35 metres (Text-fig. 4). This correlation is similar to that made between the Cismon core and La Bédoule outcrop sections, with the base of the Selli Level placed around 2.5 ‰ of $\delta^{13}C_{carb}$ (Giorgioni *et al*. 2015, fig. 6).

The dating from ammonites in Cuchía is reasonably coincident with Roquefort/La Bédoule. A *D. forbesi* Zone age is deduced from the first ammonites or the early descending interval of trough 1 at Cuchía, and a *D. weissi (forbesi)* Zone is assigned to the beginning of the same descending interval in Roquefort/La Bédoule: from metre 58 upwards to metre 56 in the section (Moullade *et al.* 2015, fig. 13). Similarly a *weissi* age is assigned to the beginning of a descending trend at metre 49 of the La Bédoule section (outcrop, not core) in Kunht *et al*. (1998, their fig. 5). Higher up in both La Bédoule sections (outcrop and core) the age is *D. deshayesi* Zone for the first through, the central plateau and the second trough of the carbon-isotope curve. This approximate biostratigraphic age match supports the geochemical correlation of the double trough of both Cuchía and Roquefort/La Bédoule and with those of Cismon core and DSDP site 463 (Text-fig. 4).

The correlation made by Lorenzen *et al.* (2013) and Moullade (2015) with Cismon is different to what we propose here. They correlate their double spike, between the heights of 30 m and 40 m, to segment C3 of Menegatti *et al*. (1998), and date it towards the middle part of the *D. deshayesi* Zone. It is made equivalent to the lower part of Cismon´s CIE.

In our interpretation segment C3 is dated as *D. forbesi* Zone. The peak negative trough-1, between segments C3-C4, is just at the base of the *D. deshayesi* Zone. Segment C4 corresponds to the *D. deshayesi* Zone, *Cheloniceras parinodum* Subzone (Text-fig. 2), and finally segment C5 (a, b) and C6 are dated *D. deshayesi* Zone, *grandis* Subzone.

The structure of the double trough has been reported in Weissert and Lini (1991), Ferreri *et al*. (1997), Grötsch *et al*. (1998), Moullade *et al*. (1998a), Renard *et al*. (2005), Najarro *et al.* 2011, Millán *et al.* (2011) and Lorenzen *et al.* (2013). However as we have shown for the Cuchía and Roquefort-La Bédoule sections, the double spike in the upper trough had never been reported and it may confuse equivalencies unless a good biostratigraphic control by ammonites supports correlation.

In conclusion, in thick neritic sections of the northern Tethys such as Roquefort/La Bédoule or Cuchía, and in thin pelagic sections of the southern Tethys or the Pacific such as Cismon and DSDP site 463 respectively, the $\delta^{13}C_{carb}$ negative flexure of the OAE 1a is characterized by two negative troughs separated by a central plateau, with a double negative spike in the upper trough of the northern Tethys sections. The double trough structure is also present in the North-Atlantic Hole 641C core (Tremolada *et al*. 2006).

### Cuchía and the Boreal OAE1a

In more northerly latitudes, the OAE1a has been reported in the Lower Saxony Basin (Germany) and the Volga Region (Russia). Ammonites from the Alstätte section (Germany) date the OAE1a equivalent in the *Deshayesites fissicostatus* Zone, the first Zone of the Early Aptian (Lehmann *et al.* 2012). On biostratigraphic grounds, this interval is correlatable with the earliest pre-OAE1a facies of the Cuchía section. In the Ulyanovsk area (Volga Region, Russia), a section interval with bituminous shale from ammonites Deshayesitid *volgensis* Zone (transition *schlovkensis-Matheronianum* Ancyloceratid Zones) is attributed to the OAE1a (Zakharov *et al.* 2013). That shale unit would be correspondent with at least part of the OAE1a represented in Cuchía. Recent work on the Eastern Russian Platform places Early Aptian OAE1a bituminous shales within the Deshayesites volgensis ammnonite range, although in the Nizhnij Lomov section the bituminous shale contains *D. deshayesi* (Zorina 2014).

## BLACK SHALES IN THE OAE1a

Black shale beds associated with OAE1a appear at different heights in the C-isotope curves for different sections. This variability seems associated with the different sedimentary, tectonic or diagenetic characteristics of each section. In a recent paper, Giorgioni *et al.* (2015) describe black-shale accumulations of both pre-OAE1a and OAE1a times in four pelagic sections of the southern and northern margins of the Alpine Tethys Ocean.

The expanded section of Cuchía and its excellent correlation with the Cismon type section has permitted the correlation of groups of black shale beds with particular segments of the OAE1a C-isotope curve. This has revealed for the first time a parallel behaviour in both pelagic and neritic environments, with respect to the TOC record variations in time.

Data from the Livello Selli equivalent in the Cismon section (northern Italy) and Roter Sattel section (western Switzerland) show two main positive shifts in the $\delta^{13}C_{carb}$ and $\delta^{13}C_{org}$ records (C4 and C6 segments), respectively in the lower and upper parts of the Selli Level interval (Menegatti *et al.* 1998).

In the Cismon core (Erba *et al.* 1999; Erba *et al*. 2010, Fig.1A; Bottini *et al*. 2013), two main intervals with black shale beds appear within the Selli level. One of them is in the lower part (CIE) and the other is in the upper part (Text-fig. 4). Both of them mostly coincide with corresponding rising trends of the $\delta^{13}C_{carb}$ curve. The lower black shale association consists of two other minor intervals enriched in organic matter, one in the lower part of the CIE and the other inmediately overlying the CIE (Text-fig. 4, right part).

In DSDP site 463 two intervals with TOC enrichment (over 5%) similarly stand out within the OAE1a around metres 615 and 620, respectively (Bottini *et al*. 2013, fig. 1). Approximately, both these intervals follow vertically two respective shifts towards positive values of the $\delta^{13}C_{carb}$ curve.

The same trend is recognized in Cuchía (Text-fig. 2). The rising TOC values at the heights 37 m and 80 m of this section appear just along the two positive shifts of the carbon-isotope curve, which succeed the two negative spikes located at respectively 34 m and 75 m (Text-fig. 2).

In summary, despite the very low relative concentration of TOC in thick neritic sections such as Cuchía, a careful C-isotope correlation with the reference section of the Selli Level (Cismon core) and DSDP site 463 in the Pacific Ocean, reveals that the main increments of organic matter preserved in the three sites were related to positive shifts of the C-isotope curve of the OAE1a. Therefore, apart from the enhancing influence of global causes such as precession-controlled black shale formation or other local causes such as basins controlled by structural highs (e.g. Giorgioni *et al*. 2015), the ultimate control in organic matter accumulation of the entire OAE1a record is oceanographic, related to intense volcanism (Ontong-Java Plateau, Bottini *et al*. 2013).

## TOC VARIATIONS (CUCHÍA, IGARATZA, IRIBAS)

We report here low TOC record and minimum TOC value oscillations with time, along with the corresponding negative shifts of their respective $\delta^{13}C_{carb}$ curves, in three sections covering the entire BCB: Cuchía (this paper), Igaratza and Iribas (García-Mondéjar *et al*. 2009) (Text-fig. 5). Correlation of the three sections has been made on biostratigraphical and geochemical evidence,

with the base of the *D. deshayesi* Zone chosen as datum. The maximum and minimum values of each curve have been outlined in order to stress the amplitudes and trends of the TOC variations with time. Common oscillations of the TOC values for the three OAE1a-equivalent succesions range from 0.2% to 0.4%. In two intervals from Cuchía and Igaratza TOC variations are very reduced and absolute values are very small (minima 1 and 2, Text-fig. 5). In Cuchía these intervals coincide approximately with descending segments of the $\delta^{13}C_{carb}$ curve of the OAE1a-equivalent (Text-figs 2 and 5); they are respectively in the lowermost part (metres 19.8 to 37.0) and in the central-upper part (metres 68.0 to 75.0) of the section. In Igaratza the TOC-minimum intervals span from metres 75.0 to 100.0 (minimum 1) and from metres 115.0 to 120.0 (minimum 2) (Text-fig. 5, centre).

A major eustatic transgression was reported in the Early Aptian (*D. forbesi* Zone, Haq *et al.* 1988, 3rd order cycle 4.1; Haq 2014, cycle KAp1). It could have resulted from oceanic capacity diminution (e.g. Pitman 1978) after massive volcanism and mid-ocean-ridge volume increments in the deep ocean (e.g. Larson and Erba 1999; Bottini *et al*. 2013). Water volume increment in the hydrosphere by volcanic outgassing could also have helped ($H_2O$ is the main volcanic gas, e.g. Symonds *et al*. 1994). Perhaps deepening of platform waters reduced shallow-water biological carbon productivity or the input of detrital organic components from continental sources.

However another possible explanation relates TOC characteristics (minima and low-amplitude variation of absolute values) with the negative shift segments of the $\delta^{13}C_{carb}$ curve. Light carbon injection from submarine volcanic source was proposed to explain the strong descending interval of the C-isotope curve at the base of the OAE1a (e.g. Méhay *et al*. 2009; Erba *et al*. 2010). Massive amounts of $CO_2$ and other greenhouse volcanic

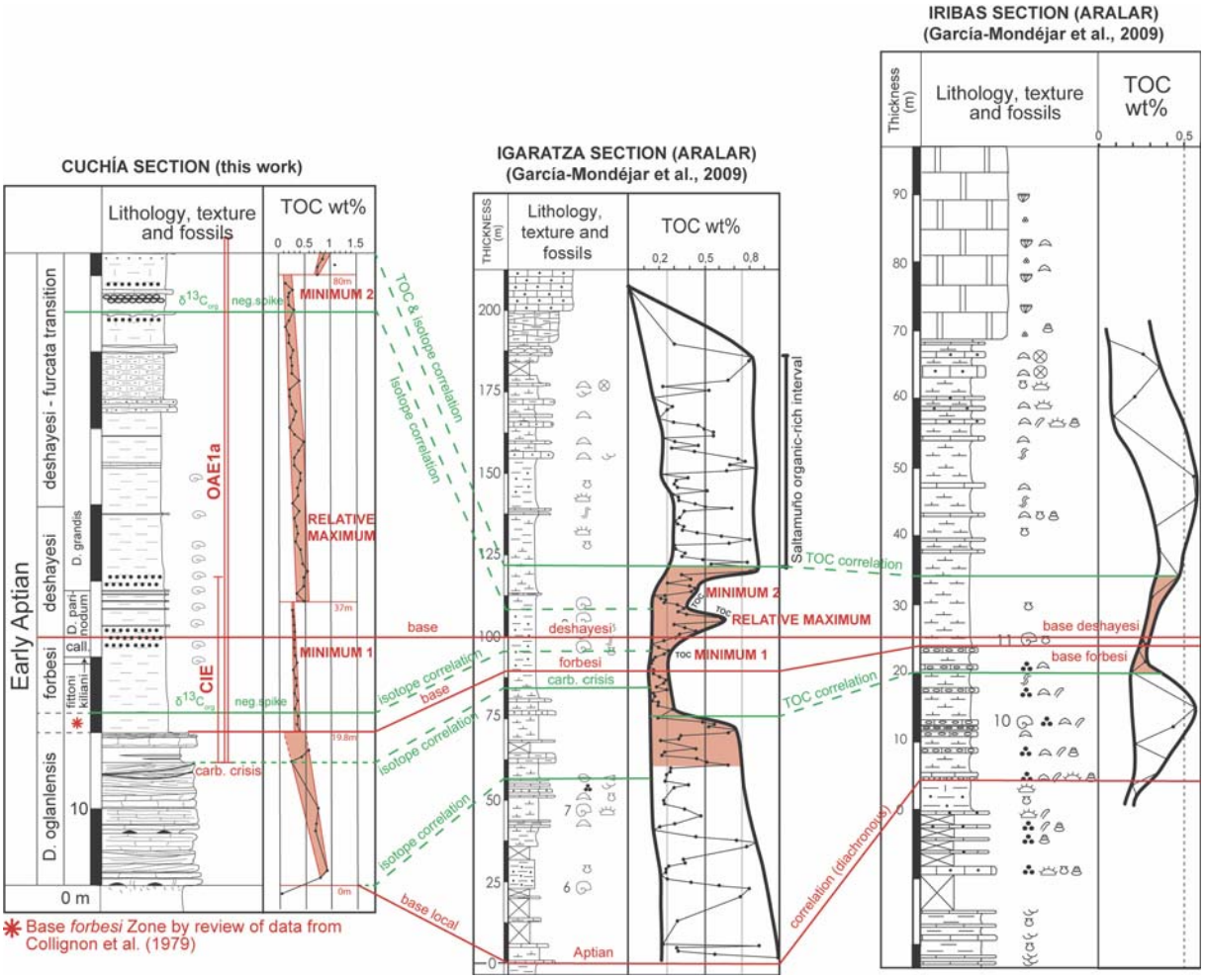


Text-fig. 5. Total organic carbon (TOC) correlation among Cuchía, Igaratza and Iribas sections in the Basque-Cantabrian basin. The base of *D. deshayesi* Zone has been chosen as datum. Different lines (C-isotopes, TOC values) complement the correlation. An interval with reduced TOC absolute values and diminished TOC variation

with time (TOC minima 1 and 2) is correlated among the three sections

gases introduced into the atmosphere would have enhanced a climatic change. Increased temperatures in the Early Aptian at the beginning of the OAE1a have been reported (e.g. Steuber *et al*. 2005; Ando *et al*. 2008; Zakharov *et al*. 2013), although accompanied by some relative colder phases (e.g. Dumitrescu *et al*. 2006; Jenkyns *et al*. 2012; Bottini *et al*. 2013; Bottini *et al*. 2015). High $CO_2$ levels in the atmosphere could have elevated polar temperatures (e.g. Barron and Washington 1982), making the world climate more uniform from the equator to the poles. This would have lowered the amplitude of climatic oscillations making a more uniform TOC record.

Large amounts of $CO_2$ in the atmosphere were also made responsible for a strong acidification in the hydrosphere and a nannoconid crisis (e.g. Erba *et al*. 2010), although they apparently did not affect organic productivity in pelagic areas (e.g. Hochuli *et al*. 1999). However acidification from these gases could have diminished the productivity in neritic areas such

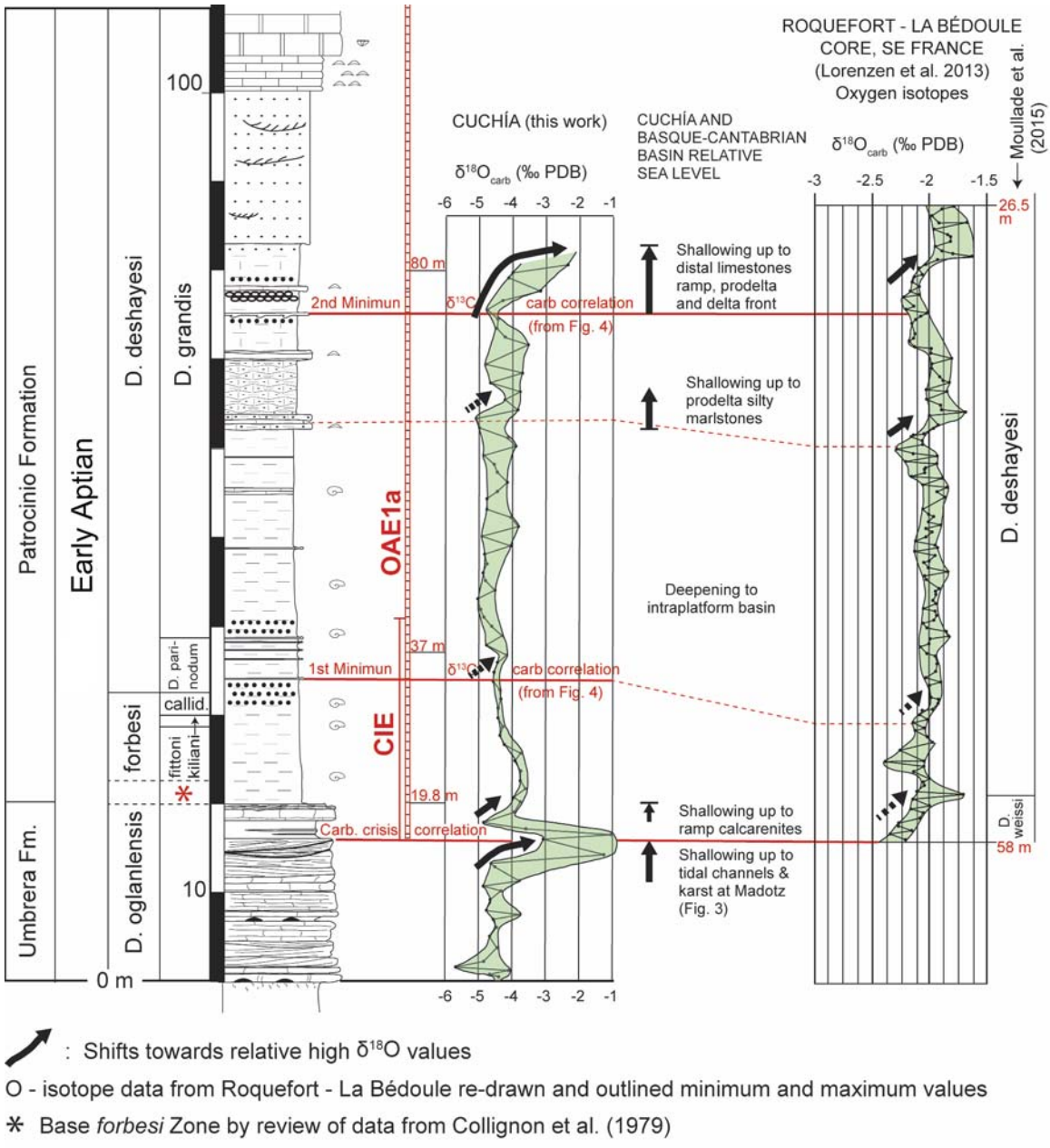


Text-fig. 6. Oxygen-isotope curve of the Cuchía section correlated with the equivalent curve from SE France (Lorenzen *et al.* 2013, modified by simplifying curve trends and introducing the two lower arrows). Positive $\delta^{18}O_{carb}$ excursions and deflections in Cuchía are correlated to SE France. Those shifts coincide with interpreted intervals of shallowing upward facies and relative sea level falls and are attributed to cooling events

as the Basque-Cantabrian, perhaps explaining the low relative values in TOC recorded in it. Carbonate platform demise (e.g. Masse and Ferneci 2011), also occurred in the BCB (e.g. Fernández-Mendiola *et al*. 2010, Millán *et al*. 2011), was probably the most relevant consequence of this acidification in neritic environments.

## OXYGEN-ISOTOPE VARIATIONS

The $\delta^{18}O$ isotope absolute values from bulk-rock of the pre- OAE1a and OAE1a-equivalent sediments in Cuchía (Menegatti´s segments C2–C6 base) are relatively low and they mostly oscillate between -4 and -5 ‰ (Text-fig. 6). Three shifts and two subtle deflections to higher values, represented with arrows, are distinguished in the curve. The first and the last shifts are the best marked (long continuous arrows). The very pronounced first shift is just below the OAE1a-equivalent interval, at top of the C2 segment (approximately at top of the *Deshayesites oglanlensis* Zone). The final major shift is already in the upper part of the OAE1a-equivalent interval, i.e. at the base of segment C6, *Deshayesites grandis* Subzone (Text-fig. 6).

The oxygen-isotope curve of the Cuchía section is correlated with a similar curve from a roughly coeval section on biostratigraphic terms (SE France, Lorenzen *et al*. 2013, fig. 4, simplified here in Text-fig. 6; Moullade *et al*. 2015, fig. 13). The main part of the compared sections belongs to the ammonites *D. deshayesi* Zone. However, the *D. weissi/D. forbesi-D. deshayesi* correlation biohorizon does not agree with the geochemical C-isotope correlation. In Cuchía this zone boundary was established with numerous specimens (see García-Mondéjar *et al*. 2015) and resulted very close to the first $\delta^{13}C_{carb}$ minimum (1.6 metres below). In Roquefort-La Bédoule the same boundary was established with very scarce and somewhat crushed ammonites specimens (Ropolo *et al*. 2006), and was placed a little more separated from the first $\delta^{13}C_{carb}$ minimum (3.5 metres below).

Three correlation horizons independent from O-isotopes are used to tie both sections: a) the carbonate crisis level (height 17 m in Cuchía, lower datum); b) the first $\delta^{13}C_{carb}$ negative spike within the lower negative trough of the OAE1a (Minimum-1, height 34 m in Cuchía, middle correlation line); and c) the uppermost of the two $\delta^{13}C_{carb}$ negative spikes within the second negative trough of the OAE1a (Minimum-2, height 75 m in Cuchía, upper datum).

The Cuchía oxygen-isotope curve shows lower absolute values than those of the similar curve from the Roquefort-La Bédoule section (SE France). The Cuchía major positive oxygen-isotope shifts are around metres 15, 19 and 80, respectively, and the little-marked positive deflections are around metres 36 and 64, respectively (Text-fig. 6). The uppermost shift (80 m) and its previous deflection (64 m) correlate with two oxygen-isotope positive shifts in SE France. In a similar way the shift at 19 m and the deflection at 36 m in Cuchía approximately correspond to the two lower shifts in the Roquefort-La Bédoule section (Text-fig. 6, arrows added in this paper). As it was mentioned before the minor discrepancy in the position of the top *D. weissi/D. forbesi* Zone between the two sections, makes correlation of this biohorizon in disagreement with the O-isotope correlation of the first shift to higher values. We attribute this to possible ammonites classification divergence owed to differences in the original materials.

The neritic Cuchía O-isotope curve is correlated with two other curves from pelagic environments: Cismon core in Italy (Erba *et al*. 2010), and DSDP Site 463 in the Pacific (Bottini *et al*. 2010). Most O-isotope trends in these curves show a close correspondence in time.

All positive O-isotope shifts in the Cuchía section except the central one at 36 m (Text-fig. 6) are related to local shallowing upward sequences (description in García-Mondéjar *et al*. 2015). Moreover the major shift in the interval 12–16 m, just below the carbonate crisis level, ends with an exposure/drowning surface that can be considered global in character. This boundary was reported with a karst surface in Aralar, 185 km to the east of Cuchía (Text-fig. 3) (top Abrevadero Member, Millán *et al*. 2011). We attrinute it to a major sequence boundary at the base of the eustatic cycle KAp1 (approximately in the transition *D. oglanlensis-D. forbesi* Zones), which involved more than 75 m of absolute sea-level fall (Haq 2014).

The uppermost shift to more positive $\delta^{18}O$ isotope absolute values in Cuchía along the 75–80 m section interval is related to a shallowing upward sequence recognized from deltaic progradation. Two more subtle equivalent sequences are present in Aralar (Igaratza and Madotz sections, Text-fig. 3), both of them located around the base of the identified Menegatti´s segment C6 as in Cuchía.

In summary, at least the two major positive shifts in $\delta^{18}O$ isotope values reported in Cuchía coincide with two respective intrabasinal shoaling upward sequences, and the older one is approximately coincident with a major eustatic sea-level fall (KAp1).

Many authors have proposed qualitative variations of climate – cooling and warming trends – based on $\delta^{18}O$ isotope analysis of bulk rock (e.g. Kunht, Holbourn and Moullade 2011; Lorenzen *et al*. 2013; Maurer *et al*. 2012; Bottini *et al*. 2015). They rely on the assumption that weak carbonate diagenesis can change the mean $\delta^{18}O$ value of a series, but usually preserves the high-frequency O-isotope variations (e.g. Stoll and Schrag 1996). In Cuchía the succesion was little tectonized, it did not reach great depths after deposition (Wilmsen 2005), and its diagenetic overprint was lessened by the high clay content.

The positive shifts in $\delta^{18}O$ isotope described in Cuchía are successfully correlated with others from contemporaneous sediments of different basins in the world using independent methods ($\delta^{13}C_{carb}$ variations, e.g. Text-fig. 6). We deduce from this fact that the main oceanographic signal of the O-isotope variations was preserved, despite the blurring effect introduced by local diagenesis.

The single major relative sea-level fall in the entire Cretaceous, that occurred approximately at the Early Aptian *D. oglanlensis-D. forbesi* transition Zone (Haq 2014, fig. 1) was accompanied by a positive shift in the $\delta^{18}O$. Among other places this shift is recorded in the Contessa section of Italy (Scrag, in Haq 2014, fig. 3). Data of the same event suggesting sea level fall and a positive $\delta^{18}O$ shift have been recognized in the Cuchía section, just before the OAE 1a record (Text-fig. 6) The other major Cuchía sea-level fall/positive shift of $\delta^{18}O$ reported here is in the *D. deshayesi* Zone and is coincident with a notable positive shift in the $\delta^{18}O$ of the Contessa section (Italy, Schrag, in Haq 2014, fig. 3), and a similar shift in Cismon core (N Italy), DSDP site 463 (Pacific) (Bottini *et al.* 2015, fig. 8), and Roquefort-La Bédoule core (Lorenzen *et al*. 2013, fig. 4).

The synchronism of relative sea-level fall-positive shift in $\delta^{18}O$ has led several authors to invoke ice accumulation on Antarctica as the primary cause of eustasy in the Cretaceous (e.g. Stoll and Schrag 1996; Miller *et al*. 2005; Immenhauser 2005). Subdued reoccurrence of eustasy in pre and late OAE1a times is likely, and could at least have happened during the two relative sea-level falls/ $\delta^{18}O$ positive shifts documented in the Cuchía section and correlated globally (top of *D. oglanlensis* Zone and middle-upper part of *D. deshayesi* Zone, respectively, Text-fig. 6)

## CONCLUSIONS

1. The Cuchía section in the western Basque-Cantabrian basin is characterized with new geochemical carbon and oxygen data. High resolution sampling along the ca. 130 m thick Early Aptian sediments has permitted the elaboration of a new $\delta^{13}C_{carb}$ curve with absolute values ranging from 4.4‰ to -2.31‰. The $\delta^{13}C_{org}$ has absolute values ranging from -27.3‰ and -22.6‰.

2. Both curves of $\delta^{13}C_{carb}$ and $\delta^{13}C_{org}$ are very much concordant. They present a wide negative excursion below followed by the rising part of a major positive excursion. These intervals are considered geochemically characteristic of the OAE1a defined from the Selli Level in Cismon core, with segments C3 to C6 equivalent to those of Menegatti *et al*. (1998).

3. Comparison with the Igaratza and Madotz sections from Aralar (eastern BCB) shows both geochemical and palaeontological concordance. All studied ammonites from Cuchía are from the lower half of the Marl Member of the Patrocinio Formation. They are dated in the *D. forbesi*, *D. deshayesi* and *D. deshayesi-D. furcata* transition Zones, which geochemically correspond to the C3-C5 segments of Menegatti *et al*. (1998).

4. Correlation of the Cuchía $\delta^{13}C_{carb}$ curve with similar curves from Cismon, Roquefort/La Bédoule and DSDP Site 463 core sections, permits the geochemical characterization of the OAE1a and its lower part (CIE) in both neritic (northern Tethys) and pelagic (southern Tethys and the Pacific) successions. The signature of these successions shows a major negative excursion in the OAE1a, consisting of a double trough separated by a flat relative maximum. The upper trough contains two negative spikes.

5. TOC analyses from the Cuchía section show absolute values ranging from 0.12% to 1.37%. These are distributed in four intervals corresponding to characteristic segments of the C-isotope curve. Intervals of major reduction in both TOC content and TOC variation amplitudes, present in Cuchía, are also common in other BCB sections (Igaratza and Iribas). Diminished productivity in neritic areas by water acidification and low seasonality by warming (greenhouse conditions) explain these geochemical variations with time.

6. $\delta^{18}O$ data in Cuchía range from -1.05‰ to -5.71‰. Background low values are punctuated by two major and three subtle shifts to higher values. Interregional correlation of the major positive shifts of Cuchía point to relative cooling periods. These shifts coincide with shallowing upward successions and relative sea-level falls.

## Acknowledgements

The project was supported by the Spanish Science and Innovation Ministry Project CGL 2009-11308, and EHU12/11 and PPM 12/11 Projects of the Basque Country University UPV/EHU. The authors thank Isabel Millán for assistance in field and laboratory work, and Sergio Hernández (UPV/EHU) for digital processing of figures. Thanks are also given to Professor J. Michalík and an anonymous reviewer for their suggestions that improved the paper.

## REFERENCES

Ando, A., Kaiho, K., Kawahata, H. and Kakegawa, T. 2008. Timing and magnitude of early Aptian extreme warming: Unraveling primary $\delta^{18}O$ variation in indurated pelagic carbonates at Deep Sea Drilling Project Site 463, central Pacific Ocean. *Palaeogeography, Palaeoclimatology, Palaeoecology*, **260**, 463–476.

Arthur, M.A. and Premoli Silva, I. 1982. Development of widespread organic carbon–rich strata in the Mediterranean Tethys. In: S.O. Schlanger and M.B. Cita (Eds), Nature and Origin of Cretaceous Carbon-Rich Facies, 75–119. Academic Press; London, New York.

Arthur, M.A., Brumsack, H.J., Jenkyns, H.C. and Schlanger, S.O. 1990. Stratigraphy, geochemistry, and paleoceanography of organic carbon-rich Cretaceous sequences. In: R.N. Ginsburg and B. Beaudoin (Eds), Cretaceous Resources, Events and Rythms, 75–119. Kluwer; Dordrecht.

Barron, E.J. and Washington, W.M. 1982. Cretaceous climate: a comparison of atmospheric simulations with the geologic record. *Palaeogeography, Palaeoclimatology and Palaeoecology,* **40**, 103–133.

Bottini, C., Cohen, A.S., Erba, E., Jenkyns, H.C. and Coe, A.L. 2013. Osmium-isotope evidence for volcanism, weathering, and ocean mixing during early Aptian OAE 1a. *Geology,* **40**, 583–586.

Bottini, C., Erba, E., Tiraboschi, D., Jenkyns, H.C., Schouten, S. and Sinninghe Damsté, J.S. 2015. Climate variability and relationship with ocean fertility during the Aptian Stage. *Climate of the Past,* **11**, 383–402.

Collignon, M., Pascal, A., Peybernès, B. and Rey, J. 1979. Faunes d'ammonites de l'Aptien de la règion de Santander (Espagne). *Annales de Paléontologie Invertébrés,* **65**, 139–156.

Dumitrescu, M., Brasell, S.C., Schouten, S., Hopman, E.C. and Sinninghe Damsté, J.S. 2006. Instability in tropical Pacific sea-surface temperatures during the early Aptian. *Geology*, **34**, 833–836.

Erba, E. 1994. Nannofossils and superplumes: the early Aptian "nannoconid crisis". *Paleoceanography,* **9**, 483–501.

Erba, E., Channel, J.E.T., Claps, M., Jones, C., Larson, R., Opdyke, B., Premoli Silva, I., Riva, A., Salvini, G. and Torricelli, S. 1999. Integrated Stratigraphy of the Cismon APTICORE (Southern Alps, Italy): a "reference section" for the Barremian–Aptian interval at low latitudes. *Journal of Foraminiferal Research,* **29**, 371–392.

Erba, E., Bottini, C., Weissert, H.J. and Keller, C.E. 2010. Calcareous nannoplankton response to surface-water acidification around oceanic anoxic event 1a. *Science,* **329** (5990), 428–432.

Erba, E., Duncan, R.A., Bottini, C., Tiraboschi, D., Weissert, H., Jenkyns, H.C. and Malinverno, A. 2015. Environmental consequences of Ontong Java Plateau and Kerguelen Plateau volcanism. In: Neal, C.R., Sager, W.W, Sano, T. and Erba, E. (Eds), The origin, evolution, and environmental impact of oceanic large igneous provinces. *Geological Society of America Special Paper*, **511**, 271–303.

Erbacher, J. and Thurow, J. 1995. A model for a sea-level controlled evolution of mid-Cretaceous black shales and Radiolaria. *Europal*, **8**, 64.

Fernández-Mendiola, P.A., García-Mondéjar, J., Millán, M.I. and Owen, H.G. 2010. Three carbonate platform episodes in the Early Aptian of N Spain. 18th International Sedimentological Congress – Mendoza, Argentina, p. 337.

Ferreri, V., Weissert, H., D'Argenio, B. and Buonocunto, F.P. 1997. Carbon isotope stratigraphy: a tool for basin to carbonate platform correlation. *Terra Nova*, **9**, 57–61.

Feuillée, P. and Rat, P. 1971. Structures et paléogéographies pyrénéo-cantabriques. In: Debyser, J., Le Pichon, X. and Montadert, L. (Eds), Colloque de l'Histoire du Golfe de Gascogne, 2, 1–45, Editions Technip; Paris.

García-Mondéjar, J. 1989. Strike-slip subsidence of the Basque-Cantabrian Basin of Northern Spain and its relationship to Aptian-Albian opening of the Bay of Biscay. In: Tankard, A.J. and Balkwill, H.R. (Eds), Extensional tectonics and stratigraphy of the North Atlantic margins. *American Association of Petroleum Geologists Memoir*, **46**, 395–409.

García-Mondéjar, J. 1990. The Aptian-Albian carbonate episode of the Basco-Cantabrian Basin (N-Spain): general characteristics, controls, and evolution. In: M.E. Tucker, M.E., Wilson, J.L., Crevello, P.D., Sarg, J.F. and Read, J.F. (Eds), Carbonate Platforms. International Association of Sedimentologists Special Publication, 9, 291–323, Blackwell; Oxford.

García-Mondéjar, J., Owen, H.G., Raisossadat, N., Millán, M.I. and Fernández-Mendiola, P.A. 2009. The Early Aptian of Aralar (northern Spain): stratigraphy, sedimentology, ammonite biozonation, and OAE1. *Cretaceous Research,* **30,** 434–464.

García-Mondéjar, J., Owen, H.G. and Fernández-Mendiola,

P.A. 2015. Early Aptian sedimentary record and OAE1a in Cuchía (Northern Spain): new data on facies and ammonite dating. *Neues Jahrbuch für Geologie und Paläontologie,* **276**, 1–26.

Giorgioni, M., Keller, C.E., Weissert, H, Hochuli, P.A. and Bernasconi, S.M. 2015. Black shales-from coolhouse to greenhouse (early Aptian). *Cretaceous Research*, **56**, 716–731.

Grötsch, J., Billing, I. and Vahrenkamp, V. 1998. Carbon-isotope stratigraphy in shallow-water carbonates: implications for Cretaceous black-shale deposition. *Sedimentology*, **45**, 623–634.

Haq, B.U. 2014. Cretaceous eustasy revisited. *Global and Planetary Change,* **113**, 44–58.

Haq, B.U., Hardenbol, J. and Vail, P.R. 1988. Mesozoic and Cenozoic chronostratigraphy and cycles of sea-level change. In: Ch.K. Wilgus, B.S. Hastings, Ch.G.St.C., Kendall, H.W. Posamentier, Ch.A. Ross, and J.C. Van Wagoner (Eds), Sea-level changes – an integrated approach. *SEPM Special Publication*, **42**, 71–108.

Heimhofer, U., Hochuli, P.A., Herrle, J.O., Andersen, N. and Weissert, H. 2004. Absence of major vegetation and palaeoatmospheric $pCO_2$ changes associated with oceanic anoxic event 1a (early Aptian, SE France*). Earth and Planetary Science Letters*, **223**, 303–318.

Herrle, J.O., Pross, J., Friedrich, O., Kössler, P. and Hemleben, C. 2003. Forcing mechanism for mid-Cretaceous black shale formation: evidence from the upper Aptian and lower Albian of the Vocontian Basin (SE France). *Palaeogeography, Palaeoclimatology Palaeoecology*, **190**, 399–426.

Hochuli, P.A., Menegatti, A.P., Weissert, H., Riva, A., Erba, E. and Silva, I.P. 1999. Episodes of high productivity and cooling in the early Aptian Alpine Tethys. *Geology,* **27**, 657–660.

Immenhauser, A. 2005. High-rate sea-level change during the Mesozoic: new approaches to an old problem. *Sedimentary Geology*, **175**, 277–296.

Jahren, A.H., Arens, N.C., Sarmiento, G., Guerrero, J. and Amundson, R. 2001. Terrestrial record of methane hydrate dissociation in the Early Cretaceous. *Geology,* **29**, 159–162.

James, N.P. and Choquette, P.W. 1990. Diagenesis 9. Limestones -the meteoric diagenetic environment. *Geoscience Canada Reprint Series,* **4**, 35–73.

Jenkyns, H.C., Schouten-Huibers, L., Schouten, S. and Sinninghe Damsté, J.S. 2012. Warm middle Jurassic-Early Cretaceous high-Latitude sea-surface temperatures from the Southern Ocean. *Climate of the Past*, **8**, 215–226.

Jones, C.E. and Jenkyns, H.C. 2001. Seawater strontium isotopes, oceanic anoxic events and sea-floor hydrothermal activity in the Jurassic and Cretaceous. *American Journal of Science,* **301**, 112–149.

Keller, C.E., Hochuli, P.A., Weissert, H., Bernasconi, S., Giorgioni, M. and Garcia, T.I. 2011. A volcanically induced climate warming and floral change preceded the onset of OAE1a (Early Cretaceous). *Palaeogeography, Palaeoclimatology, Palaeoecology*, **305**, 43–49.

Kemper, E. 1982. Zur Gliederung der Schichtfolge der Apt-Unter Alb. *Geologisches Jahrbuch, (A*) **65**, 21–33.

Kunht, W., Moullade, M., Masse J. P. and Erlenkeuser, H. 1998. Carbon isotope stratigraphy of the lower Aptian historical stratotype at Cassis-La Bédoule (SE France). *Géologie Méditerranéenne*, **25** , 63–79.

Kunht, W., Holbourn, A. and Moullade, M. 2011. Transient global cooling at the onset of the early Aptian oceanic anoxic event (OAE) 1a. *Geology,* **39**, 323–326.

Larson, R.L. and Erba, E. 1999. Onset of the mid-Cretaceous greenhouse in the Barremian- Aptian: Igneous events and the biological, sedimentary, and geochemical responses. *Paleoceanography*, **14**, 663–678.

Lehmann, J., Friedrich, O., Von Bargen, D. and Hemker, T. 2012. Early Aptian bay deposits at the southern margin of the lower Saxony Basin: Integrated stratigraphy, palaeoenvironment and OAE 1a. *Acta Geologica Polonica*, **62**, 35–62.

Lorenzen, J., Kunht, W., Holbourn, A., Flögel, S., Moullade, M. and Tronchetti, G. 2013. A new sediment core from the Bedoulian (Lower Aptian) stratotype at Roquefort-La Bédoule, SE France. *Cretaceous Research*, **39**, 6–16.

Masse, J.P. 2000. Early Aptian (112-114 Ma). In: Dercourt, J., Gaetani, M., Vrielynck, B., Barrier, E., Biju-Duval, B., Brunet, M.F., Cadet, J.P., Crasquin, S. and Sandulescu, M. (Eds), Atlas Peri-Tethys palaeogeographical maps, pp. 119–127. Gauthier-Villars; Paris.

Masse, J.P. and Fenerci-Masse M. 2011. Drowning discontinuities and stratigraphic correlation in platform carbonates. The late Barremian-Early Aptian record of southeast France. *Cretaceous Research,* **32**, 659–684.

Maurer, F., Van Buchem, F.S.P., Eberli, G.P., Pierson, B.J., Raven, M.J. and Larsen, P.H. 2012. Late Aptian long-lived glacio-eustatic lowstand recorded on the Arabian Plate. *Terra Nova,* **25**, 87–94.

Méhay, S., Keller, C.E., Bernasconi, S.M., Weissert, H., Erba, E., Bottini, C. and Hochuli, P.A. 2009. A volcanic $CO_2$ pulse triggered the Cretaceous Oceanic Anoxic Event 1a and a biocalcification crisis. *Geology,* **37**, 819–822.

Menegatti, A., Weissert, H.J., Brown, R.S., Tyson, R.V., André, P, Strasser, A. and Caron, M. 1998**.** High-resolution $\delta^{13}C$ stratigraphy through the Early Aptian "Livello Selli" of the Alpine Tethys. *Paleoceanography,* **13**, 530–545.

Mengaud, L. 1920. Recherches géologiques dans la Région Cantabrique. Thèse Faculté Science, Paris, 370 pp. Bonnet; Toulouse.

Millán, M.I., Weissert, H.J., Fernández-Mendiola, P.A. and García-Mondéjar, J. 2009. Impact of Early Aptian carbon cycle perturbations on evolution of a marine shelf system in the Basque-Cantabrian Basin (Aralar, N Spain). *Earth and Planetary Science Letters,* **287**, 392–401.

Millán, M.I., Weissert, H.J., Owen, H., Fernandez-Mendiola, P.A. and García-Mondéjar, J. 2011. The Madotz Urgonian platform (Aralar, northern Spain): Paleoecological changes in response to Early Aptian global environmental events. *Palaeogeography Palaeoclimatology Palaeoecology,* **312**, 167–180.

Miller, K.G., Wright, J.D. and Browning, J.V. 2005. Visions of ice sheets in a greenhouse world. *Marine Geology*, **217**, 215–231.

Montadert, L., Winnock, E., Deltiel, J.R. and Grau, G. 1974. Continental margins of Galicia-Portugal and Bay of Biscay. In: Burk, C.A. and Drake, C.L. (Eds), The Geology of Continental Margins, pp. 323–342. Springer; Stuttgart.

Moullade, M., Bellier, J.P. and Tronchetti, G. 2002. Hierarchy of criteria, evolutionary processes and taxonomic simplification in classification of Lower Cretaceous planktonic foraminifera. *Cretaceous Research*, **23**, 111–148.

Moullade, M., Tronchetti, G., Granier, B., Bornemann, A., Kuhnt, W. and Lorenzen, J. 2015. High-resolution integrated stratigraphy of the OAE1a and enclosing strata from core drillings in the Bedoulian stratotype (Roquefort-La Bédoule, SE France). *Cretaceous Research*, **56**, 119–140.

Najarro, M., Rosales, I. Moreno-Bedmar J.A., De Gea, G.A., Barrón, E., Company, M. and Delanoy, G. 2011. High resolution chemo- and biostratigraphic records of the Early Aptian oceanic anoxic event in Cantabria (N. Spain): palaeoceanographic and palaeoclimatic implications. *Palaeogeography, Palaeoclimatology, Palaeoecology,* **299**, 137–158.

Olivet, J.L. 1996. La cinématique de la Plaque Ibérique (Kinematics of the Iberian Plate). *Bulletin des Centres de Recherche Exploration-Production Elf Aquitaine*, **20**, 131–195.

Pitman, W.C. 1978. Relationship between eustacy and stratigraphic sequences of passive margins. *Geological Society of America Bulletin*, **80**, 1389–1403.

Premoli Silva, I., Erba, E., Salvini, G., Locatelli, C. And Verga, D. 1999. Biotic changes in Cretaceous Oceanic Anoxic Events of the Tethys. *Journal of Foraminiferal Research,* **29**, 352–370.

Renard, M., de Rafélis, M., Emmanuel, L., Moullade, M., Masse, J.P., Kuhnt, W., Bergen, J. and Tronchetti, G. 2005. Early Aptian $\delta^{13}C$ and manganese anomalies from the historical Cassis-La Bédoule stratotype sections (S.E. France): relationship with a methane hydrate dissociation event and stratigraphic implications. Carnets de Géologie/Notebook on Geology, 2005/04 (CG2005), 1–18.

Schlanger, W. and Cita, M.B. 1982. Nature and Origin of Cretaceous Carbon-Rich Facies, 229 pp. Academic Press; London, New York.

Steuber, Th., Rauch, M., Masse, J. P., Graaf, J. and Malkoc, M. 2005. Low-latitude seasonality of Cretaceous temperatures in warm and cold episodes. *Nature,* **437**, 1341–1344.

Stoll, H.M. and Schrag, D.P. 1996. Evidence for glacial control of rapid sea level changes in the early Cretaceous. *Science,* **272**, 1771–1774.

Symonds, R.B., Rose, W.I., Bluth, G. and Gerlach, T.M. 1994. Volcanic gas studies: methods, results, and applications. In: M.R. Carrol and J.R. Holloway (Eds), Volatiles in Magmas. Mineralogical Society of America. *Reviews in Mineralogy*, **30**, 1–66.

Tejada, M.L.G., Suzuki, K., Kuroda, J., Mahoney, J.J., Ohkouchi, N., Sakamoto, S.A. and Tatsumi, Y. 2009. Ontong Java Plateau eruption as a trigger for the early Aptian oceanic anoxic event. *Geology,* **37**, 855–858.

Tremolada, F., Erba, E. and Bralower, T.J. 2006. Late Barremian to early Aptian calcareous nannofossil paleoceanography and paleoecology from Ocean Drilling Program Hole 641C (Galicia Margin). *Cretaceous Research*, **27**, 887–897.

Wagner, T., Wallmann, K., Stüsser, I., Herrle, J.O., and Hofmann, P., 2007. Consequences of moderate 25,000 yr lasting emission of light $CO_2$ into the mid-Cretaceous ocean. *Earth Planetary Science Letters*, **259**, 200–211.

Weissert, H. and Lini, A. 1991. Ice age interludes during the time of Cretaceous greenhouse climate. In: D.W. Müller and H.Weissert (Eds), Controversies in modern geology, pp. 173–191. Academic Press; London.

Wiedmann, J., Reitner, J., Engeser, T. and Schwentke, W. 1983. Plattentektonik, Fazies- und Subsidenzgeschichte des baskokantabrischen Kontinentalrandes während Kreide und Alt-Tertiär. *Zitteliana*, **10**, 207–244.

Wiese, F. 1995. Das mittelturone *Romaniceras kallesi*-Event im Raum Santander (Nordspanien): Lithologie, Stratigraphie, laterale Veränderung der Ammonitenassoziationen und Paläobiogeographie. *Berliner geowissenschaftliche Abhandlungen*, E **16**, 61–77.

Wiese, F. and Wilmsen, M. 1999. Sequence stratigraphy in the Cenomanian to Campanian of the North Cantabrian Basin (Cantabria, N-Spain). *Neues Jahrbuch für Geologie und Paläontologie, Abhandlungen*, **212**, 131–173.

Wilmsen, M. 1997. Das Oberalb und Cenoman im Nordkantabrischen Becken (Provinz Kantabrien, Nordspanien): Faziesentwicklung, Bio- und Sequenzstratigraphie. *Berliner geowissenschaftliche Abhandlungen*, E **23**, 1–167.

Wilmsen, M. 2005. Stratigraphy and biofacies of the Lower

Aptian of the Cuchia (Cantabria, northern Spain). *Journal of Iberian Geology,* **31**, 253–275.

Wilpshaar, M. and Leereveld, H. 1994. Palaeoenvironmental change in the Early Cretaceous Vocontian Basin (SE France) reflected by dinoflagellate cysts. *Review of Paleobotany and Palynology*, **84**, 121–128.

Zakharov, Y.D., Baraboshkin, E.V., Weissert, H., Mikhailova, I.A., Smyshlyeva, O.P. and Safranov, P.P. 2013. Late Barremian-Early Aptian climate of the northern middle latitudes: stable isotope evidence from bivalve and cephalopod mollusks of the Russian Platform. *Cretaceous Research,* **44**, 183–201.

Zorina, S. 2014. Eustatic, tectonic and climatic signatures in the Lower Cretaceous siliciclastic succession on the Eastern Russian Platform. *Palaeogeography, Palaeoclimatology, Palaeoecology*, **412**, 91–98.

*Manuscript submitted: 15th June 2015*
*Revised version accepted: 15th November 2015*